Science in China Series G: Physics, Mechanics & Astronomy

Solidification microstructure selection of the peritectic Nd-Fe-B alloys

ZHONG Hong, LI ShuangMing†, LÜ HaiYan, LIU Lin, ZOU GuangRong & FU HengZhi

State Key Laboratory of Solidification Processing, Northwestern Polytechnical University, Xi'an 710072, China

Bridgman directional solidification and laser remelting experiments were carried out on $Nd_{11.76}Fe_{82.36}B_{5.88}$ and $Nd_{13.5}Fe_{79.75}B_{6.75}$ alloys. Microstructure evolutions along with solidification parameters (temperature gradient G, growth velocity V and initial alloy composition C_0) were investigated. A solidification microstructure selection map was established, based on the consideration of solidification characteristics of peritectic T_1 phase. In Bridgman directional solidification experiments, with the increasing growth velocities, the morphology of T_1 phase changed from plane front or faceted plane front to dendrites. In laser remelting experiments, a transition from primary γ-Fe dendrites to T_1 dendrites was found. Theoretical predictions are in good agreement with experimental results.

peritectic alloy, directional solidification, microstructure selection

Peritectic alloy has been widely used in industry, and its solidification behavior has attracted increasing attention in recent years. According to the compositional range of a peritectic phase, the peritectic alloys can be divided into two types[1]: Type A, the peritectic phase has a certain range of solubility, such as Cu-Zn, Fe-C and Fe-Ni; Type B, the solubility range of the peritectic phase is very small, such as Cu-Sn and YBCO. Magnetic material Nd-Fe-B belongs to Type B system. The superiority of Nd-Fe-B magnets mainly originates from the peritectic T_1 phase—$Nd_2Fe_{14}B$ intermetallic compound, which has a large saturation magnetization and a high anisotropy field[2]. In order to make full use of the good intrinsic properties, the volume fraction of $Nd_2Fe_{14}B$ in magnets should be maximized, and their (001) crystalline axes should be well aligned[3]. In addition to the hard magnetic T_1 phase, other nonmagnetic and soft magnetic phases also take place in the solidification of Nd-Fe-B alloys, depending on the composition and processing conditions. Therefore, better understanding and control of the solidification process must be obtained to optimize the hysteretic magnetic properties of the Nd-Fe-B alloys.

Directional solidification is an available technique to study the microstructure selection of alloys,

Received February 11, 2007; accepted April 29, 2007
doi: 10.1007/s11433-007-0041-y
†Corresponding author (email: lsm@nwpu.edu.cn)
Supported by the National Natural Science Foundation of China (Grant No. 50395100)

due to its facility of solidification parameter control. Recently, several authors[4−10] have focused on directional solidification of Type A peritectic alloys. The microstructure selection of these alloys has been successfully treated by comparing the steady state interface temperatures of competing phases. However, little attention has been devoted to Type B peritectic alloys and the solidification behavior of such alloys has not been well understood.

The aim of this study is to establish a solidification phase and microstructure selection map for Nd-Fe-B alloys at a wide range of growth velocities. Bridgman directional solidification and laser remelting experiments were carried out to evaluate the effects of composition, temperature gradient and growth velocity on the phase and microstructure selection. Solidification microstructure selection maps were presented and compared with experimental results.

1 Experiment

To investigate the solidification microstructure selection of Nd-Fe-B alloys, two types of directional solidification experiments were performed. Bridgman experiments were done at low velocities; laser remelting experiments were carried out at higher velocities.

1.1 Experimental procedure

Bridgman directional solidification experiments were undertaken for Nd-Fe-B alloys with different chemical compositions ($Nd_{11.76}Fe_{82.36}B_{5.88}$ and $Nd_{13.5}Fe_{79.75}B_{6.75}$, at%). The as-cast rod was machined to be 4 mm in diameter and 100 mm in length or 7 mm in diameter and 115 mm in length. The sample was put in an alumina crucible and solidified in a high thermal gradient Bridgman furnace[11]. The growth velocity changed from 1−300 μm/s. The sample was heated to 1400℃ and then moved through the furnace at a constant speed. After the sample reached 50 mm, the crucible was dropped into the cooling bath, in order to quench the solid/liquid interface. The mean thermal gradient, measured at different S/L interfaces with an inserted PtRh30−PtRh6 thermocouple, is shown in Figure 1. The thermal gradient decreased as the withdrawal velocity increased.

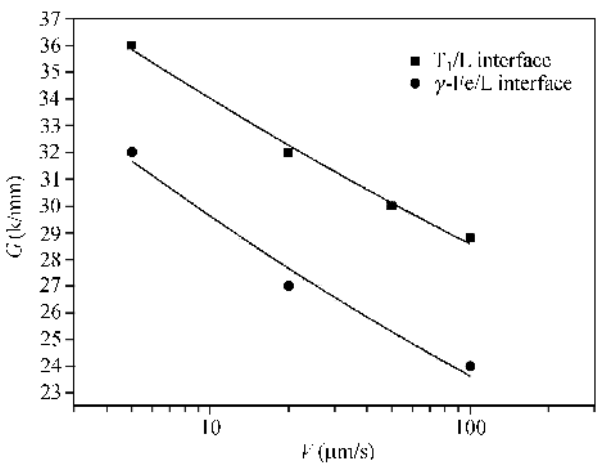

Figure 1 Dependence of temperature gradient G on withdrawal velocity V.

Laser surface remelting experiments were performed on $Nd_{13.5}Fe_{79.75}B_{6.75}$ (at%) hyperperitectic alloys. The experiments were carried out using a 5 kW continuous wave CO_2 laser (Rofin-Sinar 850)[12]. The laser beam was focused on a spot with the diameter of 0.5 mm, and a power density of 5090 $W \cdot mm^{-2}$ with the scanning velocities between 5 and 20 mm/s was obtained. The molten pool was protected by blowing a continuous flow of helium (10 min^{-1}) on the solidifying surface to prevent heavy oxidation during the laser treatment. Local growth rate V_S could be related to the scanning velocity V_b, via the expression $V_S = V_b \cos\theta$ [12], where θ is the acute angle between V_b and V_S.

All specimens were cut along the transverse and longitudinal direction, respectively. Then, the samples were polished and etched with 3% Nital to reveal the as-solidified microstructures .The microstructures were analyzed by a Leica DM4000M optical microscope.

1.2 Experimental results

Solidification microstructures consisting of primary γ-Fe (α-Fe at room temperature) dendrites, peritectic T_1 phase and black Nd-rich phase were obtained at growth rates ranging from 1 to 300 μm/s. Figure 2 shows the typical microstructures of Bridgman directional solidification samples. The S/L interface morphologies of T_1 phase at different velocities are shown in Figure 3, which changed from faceted/plane front to faceted dendrites with increasing growth rates. At withdrawal velocities between 1 and 300 μm/s, the S/L interface of γ-Fe kept dendrites (Figure 4) and always led the S/L interface of T_1 phase.

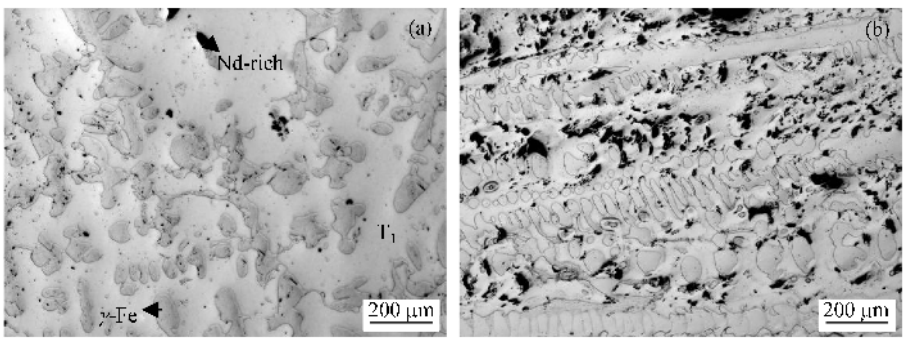

Figure 2 Optical micrograph of directionally solidified $Nd_{13.5}Fe_{79.75}B_{6.75}$ alloy, V = 2 μm/s. (a) Transverse section; (b) longitudinal section.

In laser surface remelting experiments of $Nd_{13.5}Fe_{79.75}B_{6.75}$ alloy, at growth velocity of 4.4 mm/s, the microstructures consisted of primary γ-Fe dendrites, peritectic T_1 dendrites and Nd-rich phase. At growth velocity of 5.0 mm/s, only primary T_1 faceted dendrites and Nd-rich phase were found, as shown in Figure 5.

2 Interface responses of γ-Fe and T_1 phases

The interface temperatures which, for a given alloy, are a function of composition, growth velocity and temperature gradient are called Interface Response Functions[1]. The highest interface temperature criterion is a strong indication of the structure to be formed[13].

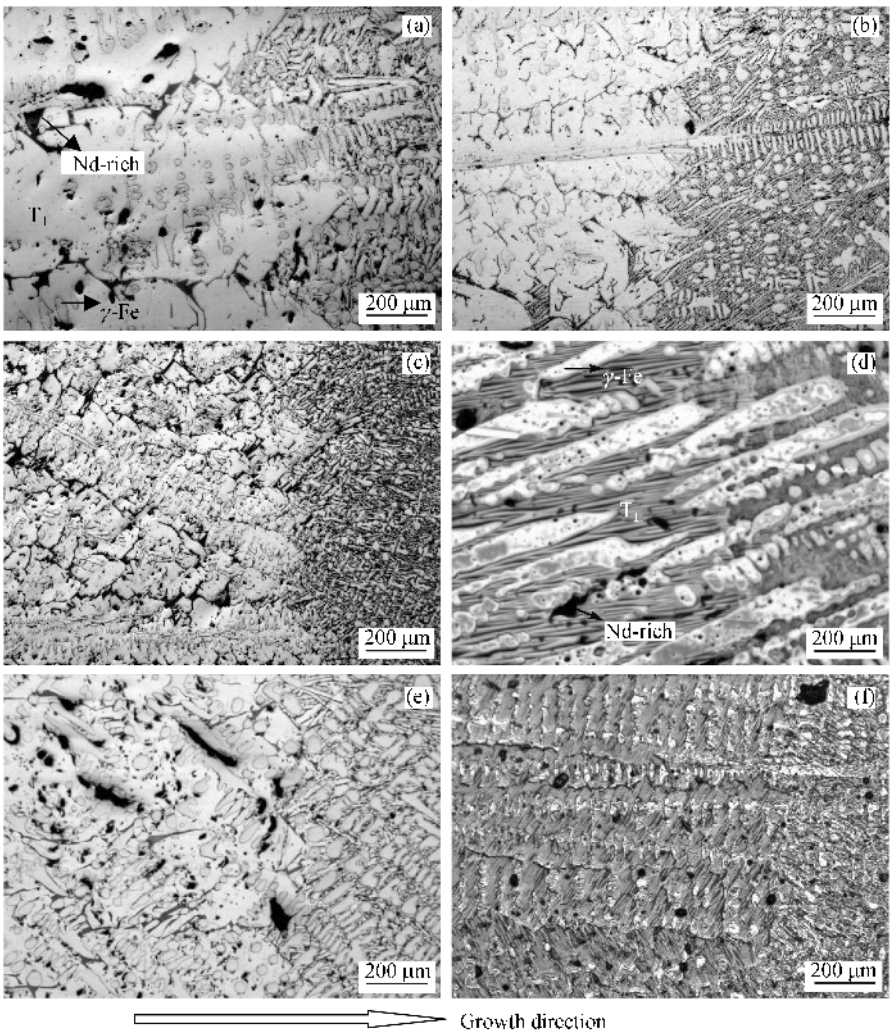

Figure 3 Dependence of T_1/L interface morphology on withdrawal velocity. (a) $Nd_{13.5}Fe_{79.75}B_{6.75}$, V = 5 μm/s; (b) $Nd_{13.5}Fe_{79.75}B_{6.75}$, V = 20 μm/s; (c) $Nd_{13.5}Fe_{79.75}B_{6.75}$, V = 50 μm/s; (d) $Nd_{11.76}Fe_{82.36}B_{5.88}$, V = 1 μm/s; (e) $Nd_{11.76}Fe_{82.36}B_{5.88}$, V = 5 μm/s; (f) $Nd_{11.76}Fe_{82.36}B_{5.88}$, V = 20 μm/s. (d), (f) Microstructures with Bitter domain observation; (a), (e) faceted plane front; (d) plane front; (b), (c), (f) dendritic interface.

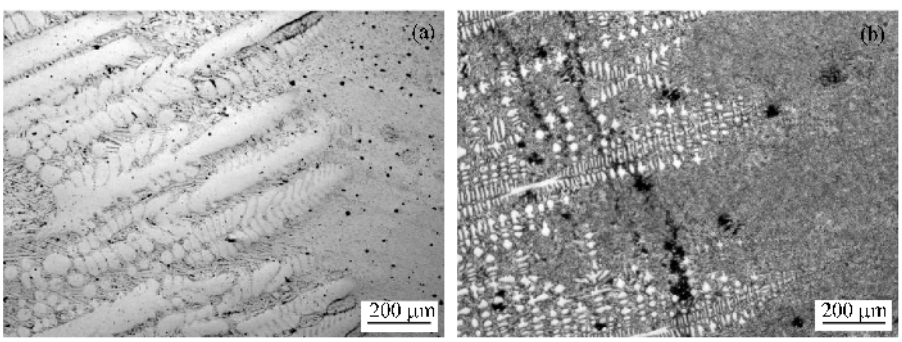

Figure 4 Microstructures observed at the solid/liquid interface of γ-Fe in directionally solidified $Nd_{11.76}Fe_{82.36}B_{5.88}$ alloy. (a) V = 1 μm/s; (b) V = 50 μm/s.

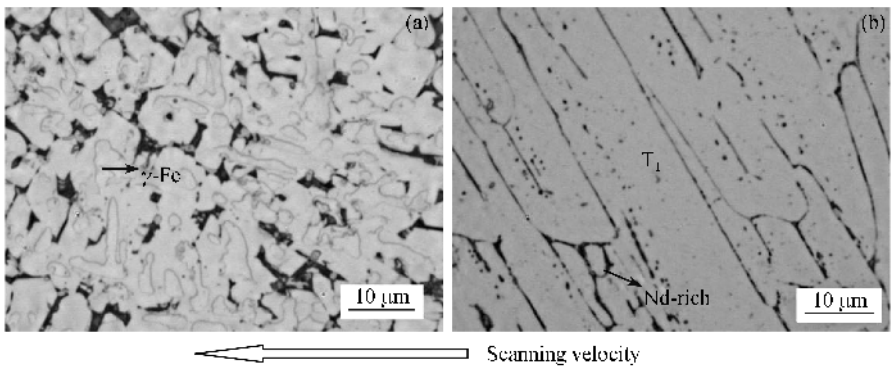

Figure 5 Typical microstructure from the longitudinal section of $Nd_{13.5}Fe_{79.75}B_{6.7}$ alloy under different solidification velocities. (a) V_b = 5 mm/s (V_S = 4.4 mm/s); (b) V_b = 10 mm/s (V_S = 5 mm/s).

As indicated in Figure 6, Nd-Fe-B phase diagram shows the following characteristics: (1) The Nd content in γ-Fe is very small; (2) the peritectic T_1 phase is an intermetallic compound which has a constant Nd content. In such a case, the interface responses (Figure 7) of γ-Fe and T_1 phases are calculated. And the velocity for a transition from one phase/morphology to another is presented below.

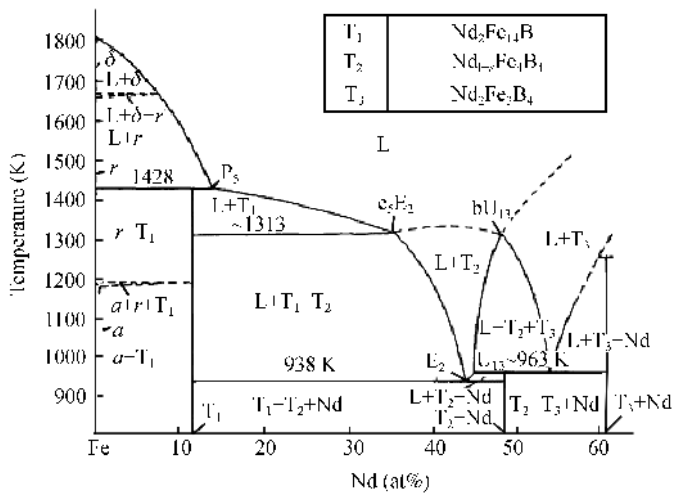

Figure 6 A vertical section of Nd-Fe-B phase diagram of Nd∶B = 2∶1[14].

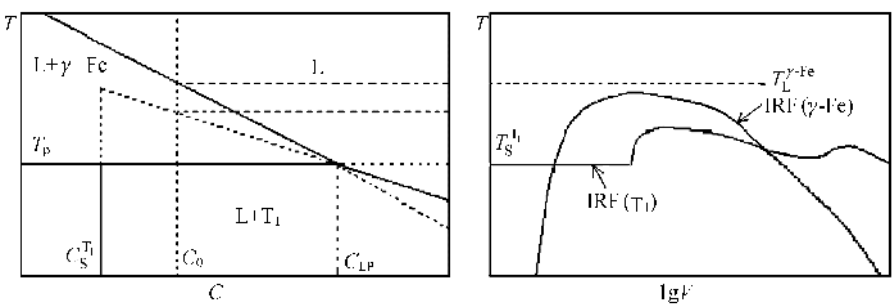

Figure 7 Schematic phase diagram for Nd-Fe-B peritectic alloy and the interface temperature changing with the growth rate.

2.1 Plane front growth at low velocities

The growth temperature of a single phase plane front is given by[13]

$$T(P) = T_S - \Delta T_k, \tag{1}$$

where T_S is the equilibrium solidus temperature; $\Delta T_k = V/\mu$ is the attachment kinetic undercooling (μ is the linear kinetic coefficient[15], and its value is in the order of 0.001—0.01 $m \cdot s^{-1} \cdot K^{-1}$ for an intermetallic alloy). Here $T(P)$ is assumed to be T_S due to a negligible attachment kinetic undercooling that is typically less than 0.1 K.

Plane front is morphologically stable at very low velocities ($V \leqslant V_C$, constitutional undercooling[16]) in directional solidification:

$$V_C = \frac{GD}{m(C_0 - C_0/k_0)}, \tag{2}$$

where D is the diffusion coefficient in liquid, m is the liquidus slope, and k_0 is the equilibrium distribution coefficient.

(i) Plane front growth of γ-Fe at low velocities. In the Nd-Fe-B phase diagram (Figure 6), $C_S^{\gamma\text{-Fe}}$ is close to zero, so that the solidification behavior of γ-Fe would be characteristic as $k_0^{\gamma\text{-Fe}} = 0$ case. Eq. (2) then predicts that $V_C^{\gamma\text{-Fe}}$ will approach zero. Therefore a plane front growth of γ-Fe would be very difficult to form.

(ii) Plane front growth of T_1 phase at low velocities. During solidification of a common alloy ($k_0 < 1$), the fully developed diffusion boundary layer was established gradually during a transient period. For T_1 phase, such a transient period would not exist. At low velocities, T_1 plane front phase has a fixed composition and it does not change with the initial alloy composition. The solute concentrations in the solid and liquid at the interface are $C_S^{T_1}$ and C_{LP}, respectively, which are independent of the original composition and keep unchanged in directional solidification, so the steady state boundary layer of T_1 phase is different from that of a common alloy, as shown in Figure 8.

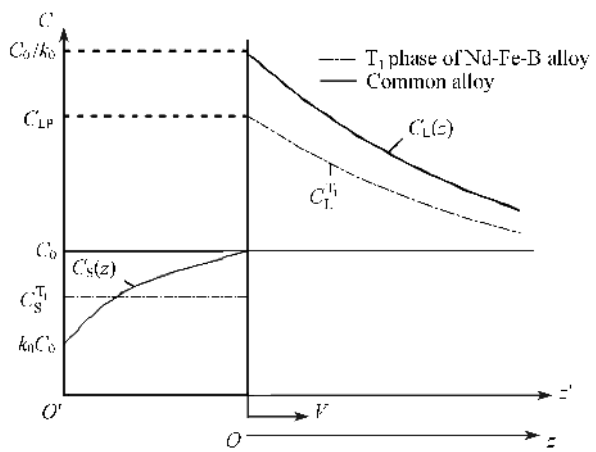

Figure 8 Steady state distribution of solute in the liquid ahead of the freezing solid-liquid interface.

The liquid solute concentration distribution ahead of a plane solid/liquid interface under steady-state conditions at low velocities could be expressed in an exponential form[16]. For T_1 phase,

it could be expressed as

$$C_{\mathrm{L}}(z) = C_0 + (C_{\mathrm{LP}} - C_0)\exp\left(-\frac{V}{D}z\right), \tag{3}$$

where C_{LP} is the liquid concentration at the peritectic temperature T_{P} (Figure 7).

Therefore, the constitutionally undercooled would not occur when eq. (4) is satisfied:

$$V \leqslant V_{\mathrm{C}}^{\mathrm{T_1}} = \frac{GD}{m(C_0 - C_{\mathrm{LP}})}. \tag{4}$$

Now compare eq. (4) with eq. (2). The $m(C_0\text{-}C_0/k_0)$ term in eq. (2) indicates the crystallization temperature interval for an alloy of composition C_0; the $m(C_0\text{-}C_{\mathrm{LP}})$ term in eq. (4) denotes the temperature interval between the extended liquidus temperature of $\mathrm{T_1}$ phase and the peritectic temperature for an alloy of composition C_0.

2.2 Competition growth between γ-Fe and $\mathrm{T_1}$ dendrites

Umeda et al.[1] have studied the phase selection of Nd-Fe-B alloys at high velocities. Critical velocities for transition from γ-Fe to $\mathrm{T_1}$ dendrites have been calculated in their paper. But the solidification characteristic of $\mathrm{T_1}$ phase was not considered.

During directional solidification, the growth temperature of a dendrite is often written as[16]

$$T_{\mathrm{d}} = T_{\mathrm{l}} - \Delta T, \tag{5}$$

where T_{l} is the liquidus temperature.

At the same time, tip undercooling for columnar dendrites can be expressed by

$$\Delta T = \Delta T_{\mathrm{C}} + \Delta T_{\mathrm{r}}, \tag{6}$$

where ΔT_{r} is the curvature undercooling, the value of which is typically in the order of $0.01-0.1$ K so that it could be neglected. At small Péclet number ($P = VR/2D$), expression for the solute undercooling ΔT_{C} is

$$\Delta T_{\mathrm{C}} = m(C_0 - C_{\mathrm{l}}^*) \cong -mC_0\Omega p, \tag{7}$$

where $p=1-k_0$; Ω is the solutal supersaturation,

$$\Omega = \frac{C_{\mathrm{LP}} - C_0}{C_{\mathrm{LP}} - C_{\mathrm{S}}^{\mathrm{T_1}}} = \frac{C_{\mathrm{LP}} - C_0}{C_{\mathrm{LP}}p}. \tag{8}$$

In this paper, $k_0^{\mathrm{T_1}}$ refers to the distribution coefficient at interface,

$$k_0^{\mathrm{T_1}} = k_{\mathrm{i}}^{\mathrm{T_1}} = C_{\mathrm{S}}^{\mathrm{T_1}} / C_{\mathrm{LP}}. \tag{9}$$

Note that, for a common alloy, the $-mC_0p$ term in eq. (7) is often substituted by $\Delta T_0 k_0$ [16]; but for $\mathrm{T_1}$ phase of Nd-Fe-B alloy, $-mC_0p$ is not the same as $\Delta T_0 k_0$.

For the supersaturation $\Omega \sim 2P$ (when P is small)[1], eq. (7) becomes

$$\Delta T_{\mathrm{C}} \cong -mC_0 pRV / D. \tag{10}$$

Here ΔT_{C} is the solute undercooling with $G = 0$. For alloys, the dendrite tip radius can be expressed as

$$R \cong \left(\frac{\Gamma D}{-mC_0 p\sigma^* V}\right)^{1/2}, \tag{11}$$

where $\sigma^* = 1/(4\pi^2)$, and Γ is the Gibbs-Thomson coefficient. Substituting eq. (11) into (10) leads to

$$\Delta T_{\mathrm{C}} \cong \left(\frac{-mC_0 p\Gamma V}{\sigma^* D} \right)^{\frac{1}{2}}. \tag{12}$$

The dendrite tip temperatures of γ-Fe and T_1 phase can thus be expressed as

$$T_{\mathrm{d}}^{0,i} = T_{\mathrm{l}} - \Delta T_{\mathrm{C}}^{0,i} = T_{\mathrm{P}} - m_i(C_0 - C_{\mathrm{P}}) - \Delta T_{\mathrm{C}}^{0,i},\ (i = \gamma\text{-Fe}, \mathrm{T_1}). \tag{13}$$

At lower velocities, the cellular interface growth temperatures can be described as[1]

$$T_{\mathrm{d/c}}^{i} = T_{\mathrm{d}}^{0,i} - G_i D / V. \tag{14}$$

Using eqs. (12)—(14), the growth interface temperatures for cellular or dendritic γ-Fe and T_1 phases can be calculated.

3 Microstructure selection map

As shown in Figure 1, the relation between temperature gradient $G_{\mathrm{T_1}}$ and withdrawal velocity V can be fitted by

$$G_{\mathrm{T_1}} = 14330 \times V^{-0.075}. \tag{15}$$

Substituting eq. (15) into (4) and using the physical constants given in Table 1, critical velocities for T_1 phase transition from plane front to cellular/dendritic growth have been calculated. For $Nd_{11.76}Fe_{82.36}B_{5.88}$ and $Nd_{13.5}Fe_{79.75}B_{6.75}$ alloys, the calculated values are 7.0×10^{-6} m/s and 1.4×10^{-5} m/s, respectively.

Table 1 Physical constants of Nd-Fe-B

Symbol	Unit	Parameter	γ-Fe	T_1	Ref.
m	K/at%	liquidus slope	−16.5	−7.7	[1]
Γ	mK	Gibbs-Thomson coefficient	2×10^{-7}	1×10^{-6}	[1]
D	m^2/s	diffusion coefficient of Nd in liquid	5×10^{-9}	5×10^{-9}	[1]
k_0		distribution coefficient		0.784	eq. (9)
C_{S}	at%	composition of solid phase		11.78	[17]
C_{LP}	at%	composition of L at T_{P}	15		[17]
T_{P}	K	peritectic temperature	1453		[17]

The $G/V_{\mathrm{C}}^{\mathrm{T_1}}$ values for various Nd contents of a constant ratio of Nd/B = 2 were calculated using eq. (4), as shown in Figure 9(a). It can be seen that the experimental data match well with the calculated values.

Although the kinetic undercooling may not affect the value of $V_{\mathrm{C}}^{\mathrm{T_1}}$, it has effects on the competition between different crystal faces of T_1 phase at velocities $V < V_{\mathrm{C}}^{\mathrm{T_1}}$, so that in directional solidification experiments, T_1 phase exhibited a plane front or faceted plane front morphology at low rates.

Figure 10 shows the calculated interface response functions for $Nd_{11.76}Fe_{82.36}B_{5.88}$ and $Nd_{13.5}Fe_{79.75}B_{6.75}$ alloys. The calculated V_{tr} for the two alloys are 3.2×10^{-3} m/s and 5.9×10^{-3} m/s, respectively. At growth rates $V < V_{\mathrm{tr}}$, γ-Fe would grow as the primary phase; at $V > V_{\mathrm{tr}}$, T_1 faceted dendrites would become the leading morphology.

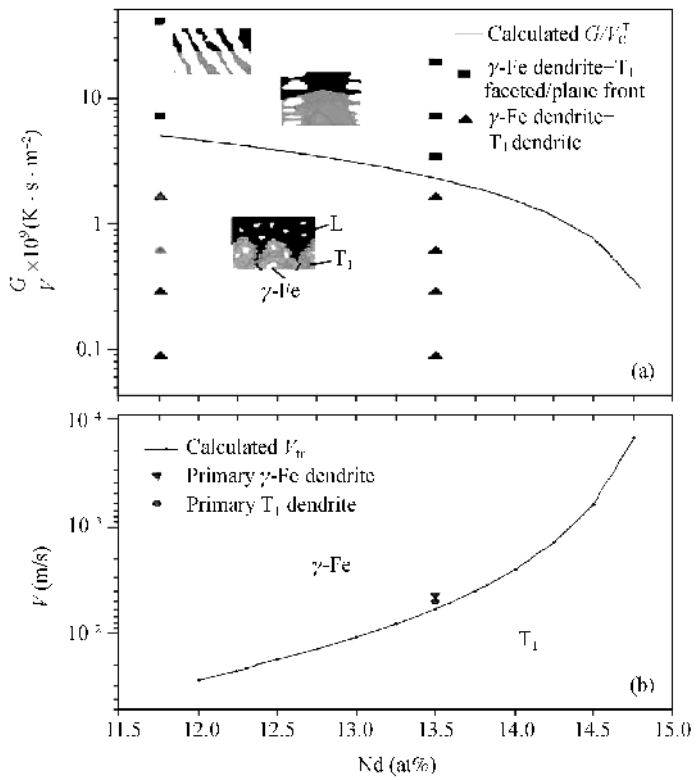

Figure 9 Solidification microstructure selection map of Nd-Fe-B.

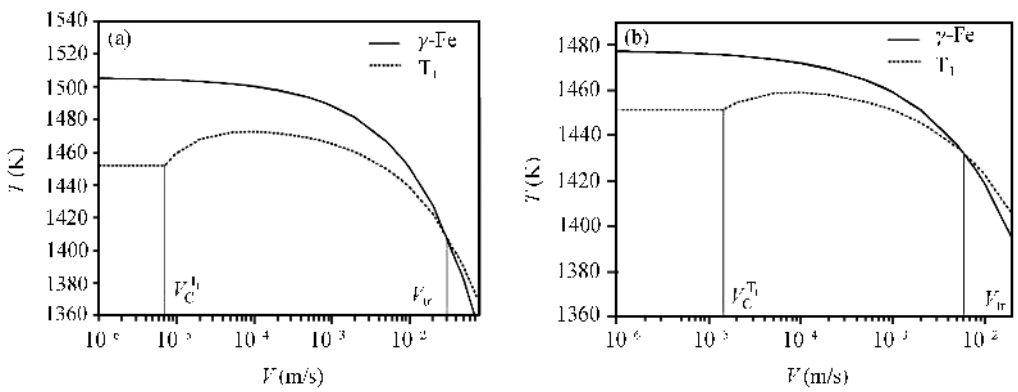

Figure 10 Interface temperatures of γ-Fe and T_1 phases in Nd-Fe-B at different growth rates. (a) $Nd_{11.76}Fe_{82.36}B_{5.88}$; (b) $Nd_{13.5}Fe_{79.75}B_{6.75}$.

Critical velocities for the phase transition from γ-Fe dendrites to T_1 dendrites with different Nd contents are shown in Figure 9(b). The predicted values of V_{tr} are higher than that reported by Umeda et al.[1] (For $Nd_{13.5}Fe_{79.75}B_{6.75}$ alloy, the value of V_{tr} in their paper is about 1×10^{-3} m/s, which is about one sixth of the value in this paper). From the laser surface remelting experiments, the value of V_{tr} for $Nd_{13.5}Fe_{79.75}B_{6.75}$ alloy was investigated to be in the range between 4.4×10^{-3} m/s and 5.0×10^{-3} m/s, which is in approximate agreement with the calculated value, as shown in Figure 9(b).

Figure 9(a) and (b) gives the microstructure selection map of Nd-Fe-B alloys with peritectic and

hyperperitectic compositions, containing plane front at low velocities and dendritic morphologies at higher velocities.

4 Conclusions

(1) Critical velocities $V_C^{T_1}$ for the T_1 phase transition from plane front to cellular/dendrite interface have been calculated. The values of $Nd_{11.76}Fe_{82.36}B_{5.88}$ and $Nd_{13.5}Fe_{79.75}B_{6.75}$(at%) alloys are 7.0×10^{-6} m/s ($G = 349$ K/cm) and 1.4×10^{-5} m/s ($G = 331$ K/cm), respectively. In Bridgman directional solidification experiments, with increasing growth velocities, T_1 phase changed from plane front or faceted plane front to faceted dendrites. The experimental results are in good agreement with the calculated values.

(2) Critical velocities V_{tr} for transition from primary γ-Fe dendrites to T_1 dendrites were calculated. The value of V_{tr} for $Nd_{13.5}Fe_{79.75}B_{6.75}$ (at%) alloy is 5.9×10^{-3} m/s. During laser remelting experiments, V_{tr} for $Nd_{13.5}Fe_{79.75}B_{6.75}$ alloy was investigated to be in the range between 4.4×10^{-3} m/s and 5.0×10^{-3} m/s. The experimental result is in reasonable agreement with the calculated value.

(3) A microstructure selection map for Nd-Fe-B alloys was presented using both the criterion of the highest interface temperature and directional solidification experimental results.

1 Umeda T, Okane T, Kurz W. Phase selection during solidification of peritectic alloys. Acta Materialia, 1996, 44: 4209－4216
2 Ozawa S, Saito T, Motegi T. Effects of cooling rate on microstructures and magnetic properties of Nd-Fe-B alloys. J Alloys Compds, 2004, 363: 263－270
3 Ozawa S, Saito T, Yu J, et al. Solidification behavior in undercooled Nd-Fe-B alloys. J Alloys Compds, 2001, 322: 276－280
4 Huang W D, Lin X, Wang M, et al. Pattern and phase selection of peritectic reaction during directional solidification. Sci China Ser E-Eng Mater Sci, 2002, 45(5): 458－466
5 Xu W, Feng Y P, Li Y, et al. Rapid solidification behavior of Zn-rich Zn-Ag peritectic alloys. Acta Materialia, 2002, 50: 183－193
6 Trivedi R, Park J S. Dynamics of microstructure formation in the two-phase region of peritectic systems. J Cryst Growth, 2002, 235: 572－588
7 Lo T S, Dobler S, Plapp M, et al. Two-phase microstructure selection in peritectic solidification: From island banding to coupled growth. Acta Materialia, 2003, 51: 599－611
8 Lograsso T A, Fuh B C, Trivedi R. Phase selection during directional solidification of peritectic alloys. Metall Mater Trans, 2005, 36: 1287－1300
9 Su Y Q, Liu C, Li X Z, et al. Microstructure selection during the directionally peritectic solidification of Ti-Al binary system. Intermetallics, 2005, 13: 267－274
10 Ma D, Li Y, Ng S C, et al. Unidirectional solidification of Zn-rich Zn-Cu peritectic alloys (I): Microstructure selection. Acta Materialia, 2000, 48: 419－431
11 He Q, Liu L, Zou G R, et al. Investigation of microstructure of Nd-Fe-B peritectic alloys under directional solidification. J Mater Eng, 2004, 6: 17－19
12 Su Y P, Lin X, Wang M, et al. Lamellar structures in laser surface remelted Zn-Cu peritectic alloy under ultra-high temperature gradient. Scripta Materialia, 2004, 51: 397－403
13 Kurz W. Solidification microstructure processing maps: Theory and application. Adv Eng Mater, 2001, 7: 443－452
14 Matsuura Y, Hirosawa S, Yamamoto H, et al. Phase diagram of the NdFeB ternary system. Jpn J Appl Phys, 1985, 24: 635－638
15 Li J F, Zhou Y H. Effect of interface kinetics on the eutectic growth. Sci China Ser E-Eng Mater Sci, 2005, 48(4): 361－371
16 Kurz W, Fisher D J. Fundamentals of Solidification. 4th ed. Switzerland: Trans Tech Publications Ltd., 1998. 54－240
17 Zhou S Z, Dong Q F. Super Permanent Magnet－Rare Earth Iron Series Permanent Magnet Material. 2nd ed. Beijing: Metallurgical Industry Press, 2004. 84－91